Novel Conotoxins from *Conus striatus* and *Conus kinoshitai* Selectively Block TTX-Resistant Sodium Channels†

Grzegorz Bulaj,*,‡,§,|| Peter J. West,‡,|| James E. Garrett,§ Maren Watkins,⊥ Min-Min Zhang,‡ Raymond S. Norton,@ Brian J. Smith,@ Doju Yoshikami,‡ and Baldomero M. Olivera‡

Departments of Biology and Pathology, University of Utah, Salt Lake City, Utah 84112, Cognetix, Inc., 421 Wakara Way, Suite 201, Salt Lake City, Utah 84108, and The Walter and Eliza Hall Institute of Medical Research, 1G Royal Parade, Parkville 3050, Australia

Received December 18, 2004; Revised Manuscript Received March 24, 2005

ABSTRACT: The peptides isolated from venoms of predatory marine *Conus* snails ("conotoxins") are well-known to be highly potent and selective pharmacological agents for voltage-gated ion channels and receptors. We report the discovery of two novel TTX-resistant sodium channel blockers, μ-conotoxins SIIIA and KIIIA, from two species of cone snails. The two toxins were identified and characterized by combining molecular techniques and chemical synthesis. Both peptides inhibit TTX-resistant sodium currents in neurons of frog sympathetic and dorsal root ganglia but poorly block action potentials in frog skeletal muscle, which are mediated by TTX-sensitive sodium channels. The amino acid sequences in the C-terminal region of the two peptides and of the previously characterized μ-conotoxin SmIIIA (which also blocks TTX-resistant channels) are similar, but the three peptides differ in the length of their first N-terminal loop. We used molecular dynamics simulations to analyze how altering the number of residues in the first loop affects the overall structure of μ-conotoxins. Our results suggest that the naturally occurring truncations do not affect the conformation of the C-terminal loops. Taken together, structural and functional differences among μ-conotoxins SmIIIA, SIIIA, and KIIIA offer a unique insight into the "evolutionary engineering" of conotoxin activity.

Voltage-gated sodium channels (VGSCs)[1] are responsible for the influx of Na^+ during action potentials in excitable tissues. The α-subunits of VGSCs from a variety of organisms have been cloned, and nine subtypes have been discovered in mammals (reviewed in refs *1*−*3*). The majority of these VGSCs, including the skeletal muscle subtype, are inhibited by tetrodotoxin (TTX) at concentrations in the low nanomolar range. In contrast, two of the subtypes are highly resistant to TTX with IC_{50} values of ≥50 μM, and they are primarily expressed in dorsal root ganglia (DRG) neurons (reviewed in *2*). At present, there is considerable interest in these TTX-resistant (TTX-r) sodium channels because of their potential importance in pain perception. Major efforts are being made to determine whether the TTX-r VGSCs will be useful pharmacological targets for drugs that can be developed to alleviate various pathological states such as neuropathic pain (*4*).

The venomous cone snails are a rich source of toxins that target VGSCs (*5*). Among these are peptides belonging to the μ-conotoxin family. Like TTX, μ-conotoxins inhibit sodium currents by acting at site 1 of VGSCs (see ref *6* for review). However, unlike TTX, several members of the μ-conotoxin family selectively block particular subtypes of the VGSCs. The first, and defining, members of this family were shown to preferentially block the skeletal muscle VGSC, $Na_v1.4$ (*7*−*10*). More recently, a toxin from the venom of *Conus stercusmuscarum*, μ-conotoxin SmIIIA (μ-SmIIIA), was discovered that irreversibly inhibits TTX-resistant sodium currents in amphibian sympathetic and DRG neurons (*11*). Although μ-SmIIIA had little or no effect on TTX-sensitive sodium currents and action potentials in these neurons, it reversibly inhibited TTX-sensitive action potentials in frog skeletal muscle (*12*).

In this work, we report the characterization of two novel μ-conotoxins from the venoms of two different fish-hunting species, *Conus striatus* and *Conus kinoshitai* (see Figure 1). These peptides inhibit TTX-r sodium currents in amphibian sympathetic and DRG neurons. However, in contrast to μ-SmIIIA, the new peptides are poor blockers of action potentials in frog skeletal muscle. The sequence similarities between the μ-conotoxins that inhibit TTX-r Na currents suggest structural determinants that mediate their shared ability to target TTX-r VGSCs. The sequence divergence is

† This work was supported by NIH Grant GM 48677 (to B.M.O.), from the National Institute of General Medical Sciences. B.J.S. acknowledges support from the NHMRC.

* To whom correspondence should be addressed: Department of Biology, University of Utah, 257 South 1400 East, Salt Lake City, Utah 84112. Telephone: (801) 581-8370. Fax: (801) 585-5010. E-mail: bulaj@biology.utah.edu.

‡ Department of Biology, University of Utah.

§ Cognetix, Inc.

|| These authors contributed equally to this work.

⊥ Department of Pathology, University of Utah.

@ The Walter and Eliza Hall Institute of Medical Research.

[1] Abbreviations: ACN, acetonitrile; CAP, compound action potential; DRG, dorsal root ganglia; MD, molecular dynamics; MTBE, methyl *tert*-butyl ether; μ-KIIIA, μ-conotoxin KIIIA; μ-SIIIA, μ-conotoxin SIIIA; μ-SmIIIA, μ-conotoxin SmIIIA; TFA, trifluoroacetic acid; TTX, tetrodotoxin; TTX-r, tetrodotoxin-resistant; VGSC, voltage-gated sodium channel.

10.1021/bi0473408 CCC: $30.25
Published on Web 04/21/2005

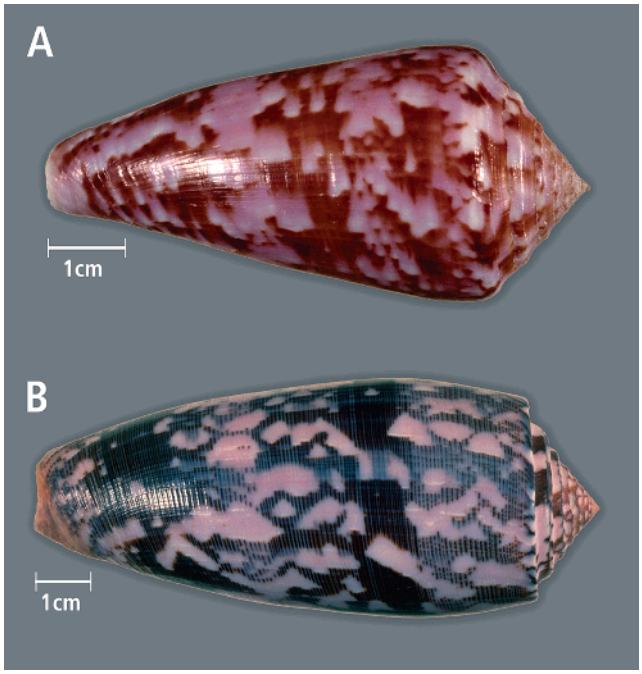

FIGURE 1: Shells from (A) *C. kinoshitai* and (B) *C. striatus*. *C. kinoshitai* is collected in deep water by trawling nets from the Philippines to Southern Japan. *C. striatus* is collected by divers in shallower water over the entire Indo-Pacific, from Hawaii to East Africa.

presumably responsible for differences in the interactions observed between the toxins and various Na^+ channel subtypes.

EXPERIMENTAL PROCEDURES

Cloning of Conotoxins. PCR amplification, construction of cDNA libraries, and cloning of μ-conotoxins were performed as described by West et al. (*11*).

Chemical Synthesis of Conotoxins. Peptides were synthesized on amide MBHA resin using standard Fmoc [*N*-(9-fluorenyl)methoxycarbonyl] chemistry. The peptides were cleaved from the resin by a 4 h treatment with reagent K [trifluoroacetic acid (TFA), water, ethanedithiol, phenol, and thioanisole, 90/5/2.5/7.5/5 by volume]. The cleaved peptides were filtered, precipitated with methyl *tert*-butyl ether (MTBE) precooled to −20 °C, and washed several times with cold MTBE. The linear peptides were purified by reversed-phase HPLC using a preparative C_{18} Vydac column (218TP1022) eluted with a linear gradient of acetonitrile (ACN) (in 0.1% TFA). The flow rate was 10 mL/min, and the elution was monitored by UV detection at 210 nm. The peptides were dried by lyophilization. Oxidative folding was performed by resuspending the linear peptides in 0.01% TFA in water and injecting the suspension into a buffered solution [0.1 M Tris-HCl (pH 7.5)] containing 1 mM EDTA, 1 mM reduced glutathione, and 1 mM oxidized glutathione. The final peptide concentration was 20 μM. Progress of the folding reaction was monitored by analytical reversed-phase HPLC using a C_{18} Vydac column (218TP54, 4.6 mm × 250 mm) eluted with a gradient of ACN at a flow rate of 1 mL/min; the eluent was monitored at 220 nm. After the completion of folding, the reaction was quenched by acidification with formic acid (8% final concentration). The peptides were repurified by semipreparative HPLC as described for the purification of the linear forms. The identity of each peptide was confirmed by MALDI-TOF mass spectrometry analysis with a Bruker Daltonics Omni FLEX spectrometer, operated in the reflectron mode. Samples were dissolved in 0.1% TFA and mixed with matrix (α-cyano-4-hydroxycinnamic acid) suspended in 70% ACN in water containing 0.1% TFA.

Electrophysiology. Lumbar paravertebral sympathetic ganglia and DRG were dissected from 2.5−3 in. adult frogs (*Rana pipiens*) of either sex and dissociated in a manner similar to that described by others (*13*, *14*). Briefly, ganglia were treated with collagenase followed by trypsin. Cells were mechanically dissociated by trituration, washed and suspended in 73% Leibowitz's L15 solution (supplemented with 14 mM glucose, 1 mM $CaC1_2$, 7% fetal bovine serum, and penicillin/streptomycin), plated on polylysine-coated coverslips, and stored at 4 °C.

Neurons were perfused with extracellular solution containing 117 mM NaCl, 2 mM KCl, 2 mM $MgCl_2$, 2 mM $MnCl_2$, 5 mM HEPES, and 10 mM TEA (pH 7.2). To record TTX-resistant currents, 1−10 μM TTX was added to the bathing solution. Recording pipets contained 10 mM NaCl, 110 mM CsCl, 2 mM $MgCl_2$, 0.4 mM $CaCl_2$, 4.4 mM EGTA, 5 mM HEPES, 5 mM TEA, and 4 mM MgATP (pH 7.2). These solutions inhibit voltage-gated potassium and calcium currents and thereby permit recording of sodium currents alone. Conotoxins were dissolved in an extracellular solution and applied to neurons under study by bath exchange. Toxin exposures were conducted in static baths. Neurons were voltage clamped in the whole-cell configuration, held at −80 mV, and VGSCs were activated by a 50 ms test pulse to 0 mV, applied every 10 s. Each test pulse was preceded by a −120 mV prepulse lasting 50 ms. Current signals, acquired at room temperature with either an Axopatch 200B or MultiClamp 700A amplifier (Axon Instruments, Union City, CA), were filtered at 2 kHz, digitized at 10 kHz, and leak-subtracted by a P/5 protocol using in-house software written in LabVIEW (National Instruments, Austin, TX).

Extracellular recordings of compound action potentials (CAPs) from frog skeletal muscle and postganglionic sympathetic nerve were made essentially as previously described (*8*, *12*, *15*, *16*). Briefly, the cutaneous pectoris muscle or lumbar sympathetic ganglia 8−10 and the adjoining 10th spinal nerve were dissected from 2.5−3 in. adult frogs (*R. pipiens*) of either sex. The muscle was trimmed longitudinally so that only ∼25−50% of the muscle remained. This muscle and sympathetic preparations were either used on the same day of dissection or refrigerated at 4 °C and used within 2 days. The trimmed muscle was pinned in a shallow rectangular recording chamber made of Sylgard (Dow Chemical, Midland, MI). The proximal end of the motor nerve innervating the muscle was draped over into a two-compartment well adjacent to the rectangular muscle compartment. For the sympathetic preparation, the recording chamber consisted of seven circular or semicircular compartments with diameters between 4 and 5 mm, each separated from its neighbor by an ∼1 mm wide partition. A bead of Vaseline was placed atop each partition between compartments. Portions of nerve draped over the Vaseline were covered with additional Vaseline to prevent drying and to seal off compartments from each other such that the fluid in each compartment was isolated and independently maintained

Table 1: μ-Conotoxins from Fish-Hunting Cone Snails[a]

Conus Species	μ-Conotoxin	Sequence	Ref
C. stercusmuscarum	SmIIIA	ZR**CC**NGRRG**C**SSR**W**C**R**DHSR**CC**#	(*11*)
C. striatus	SIIIA	ZN**CC**NG--G**C**SSK**W**C**R**DHA**R**C**C**#	this work
C. kinoshitai	KIIIA	**CC**N----**C**SSK**W**C**R**DHSR**CC**#	this work
C. purpurascens	PIIIA	ZRL**CC**GFOKS**C**RSR**Q**C**K**OH-**R**C**C**#	(*8*)
C. geographus	GIIIA	RD**CC**TOOKK**C**KDR**Q**C**K**OQ-**R**C**C**A#	(*26*)

[a] The number sign (#) denotes C-terminal amidation, Z pyroglutamate, and O hydroxyproline. The underlined Arg or Lys residue in the second loop is suggested to play a key role for the potency of these peptides.

and electrical stimulation or recording across compartment partitions was possible. Each compartment was maintained essentially as a static bath except for the test compartment, which was perfused when it did not contain toxin. For the muscle preparation, a stimulating electrode was placed in each of the two compartments of the well containing the motor nerve, while one recording electrode was placed in the middle, and the other electrode at one end, of the rectangular chamber containing the muscle. For the sympathetic preparation, a pair of electrodes provided stimuli to the preganglionic nerve between the eighth and ninth ganglia, while postganglionic CAPs were recorded from the 10th spinal nerve. All compartments contained normal frog Ringer's solution consisting of 111 mM NaCl, 2 mM KCl, 1.8 mM $CaCl_2$, and 10 mM HEPES (pH 7.2). Conotoxins were dissolved in this solution and applied to the muscle-containing compartment by replacing its solution with one containing toxin. Toxin exposures were carried out in a static bath to conserve toxin.

Skeletal muscle CAPs were evoked by stimulating the motor nerve with ~10 V, 0.1 ms rectangular pulses, and CAPs in the postganglionic nerve were evoked by stimulating the preganglionic nerve with ~20 V, 1 ms rectangular pulses, provided by an S-88 stimulator (Grass Instruments, West Warwick, RI) through a stimulus isolation unit. All electrodes were platinum wires, and all experiments were performed at room temperature. Recordings were made with a P-55 differential A/C preamplifier (Grass Instruments) with band-pass filter settings of 1 Hz and 1 kHz. Signals were digitized at a sampling frequency of 5 kHz and acquired with in-house software written in LabVIEW (National Instruments).

Data were analyzed using Graphpad Prism for Macintosh (version 3.0cx, Graphpad Software, San Diego, CA) or Kaleidagraph for Macintosh (version 3.6, Synergy Software, Reading, PA). Data are presented as the mean ± the standard error of the mean (SEM), and error bars on all graphs represent the SEM.

Molecular Modeling. Models of μ-SIIIA and μ-KIIIA were generated by comparative modeling methods (*17*) using the solution structure of μ-SmIIIA (*12*; PDB entry 1Q2J, representative structure 13) as a template. The sequence alignment present in Table 1 was used to generate 25 initial models of the structures using Modeler (6v2) (*18*). The structure with the lowest Modeler objective function was used for further analysis in each system. Molecular dynamics (MD) simulations were performed using the Gromacs version 3.1.4 package of programs (*19*) with the OPLS-aa force field (*20*). Ionizable amino acids were assumed to be in their standard state at neutral pH, while histidine was neutral [note that the pK_a of His19 in μ-SmIIIA is 6.8 (*12*)]; the C-terminus was in the amidated form, while the N-terminus was charged for μ-KIIIA and neutral (pyroGlu) for μ-SmIIIA and μ-SIIIA. Proteins were solvated in a box of water with dimensions of 40 Å; no pressure coupling was applied. The total charge on the system was made neutral by replacing water molecules with chloride ions using Genion. The LINCS algorithm (*21*) was used to constrain bond lengths. Protein, water, and ions were coupled separately to a thermal bath at 300 K using a Berendsen thermostat (*22*) applied with a coupling time of 0.1 ps. All simulations were performed with a single nonbonded cutoff of 10 Å, applying a neighbor-list update frequency of 10 steps (20 fs). The particle mesh Ewald method was applied to deal with long-range electrostatics with a grid width of 1.2 Å and fourth-order spline interpolation. All simulations consisted of an initial minimization to prevent close contacts, followed by 10 ps of "positional restrained" MD to equilibrate the water molecules (with the polypeptide fixed). The time step used in the simulations

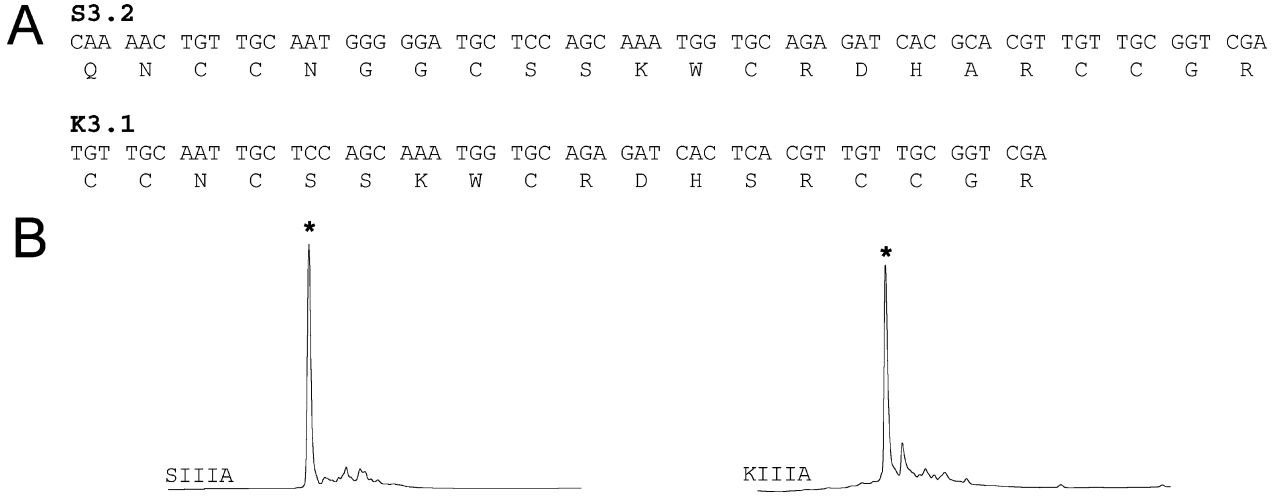

FIGURE 2: Identification and chemical synthesis of μ-conotoxins SIIIA and KIIIA. (A) Relevant nucleic acid sequence and the translated amino acid sequence from *C. striatus* and *C. kinoshitai*. The predicted mature conotoxin sequences (assuming the C-terminus was processed from C-G-R to C-NH_2) were chemically synthesized and oxidized in the presence of glutathione. (B) HPLC analysis of the oxidative folding of μ-SIIIA and μ-KIIIA. The major oxidation product, indicated by the asterisk, was purified and used for further characterization.

was 2 fs. Each MD simulation was run for a total length of 10 ns. At the completion of the MD simulation, each system was minimized using the method of steepest descents.

RESULTS

Identification of Cloned Sequences Encoding Novel μ-Conotoxins from C. striatus and C. kinoshitai. To identify μ-conotoxins that might exhibit subtype specificity for TTX-r VGSCs, we carried out a survey of cDNA sequences obtained from the venom ducts of various fish-hunting *Conus* species that encoded peptides of the μ-conotoxin family. Two cDNA sequences, one from *C. striatus*, a well-known fish-hunting *Conus* species from shallow waters in the Indo-Pacific, and the other from *C. kinoshitai*, a putative fish-hunting species generally collected in deeper waters (>100 m) from the Southern Philippines to Southern Japan (see Figure 1), seemed to be particularly promising. The predicted AA sequences from the cDNA clones (Figure 2A) exhibit strong sequence similarity to the recently characterized *C. stercusmuscarum* peptide μ-SmIIIA (*11*), and are much less homologous to μ-conotoxins primarily targeted to the muscle subtype of VGSCs, such as μ-conotoxin GIIIA (μ-GIIIA) from *Conus geographus* (*7*) and μ-conotoxin PIIIA (μ-PIIIA) from *Conus purpurascens* (*8*). We designate the peptides from *C. striatus* and *C. kinoshitai* μ-conotoxin SIIIA (μ-SIIIA) and μ-conotoxin KIIIA (μ-KIIIA), respectively.

Chemical Synthesis and Mass Spectrometry. The predicted conotoxins were chemically synthesized by standard solid-phase methods. The linear forms were allowed to fold in the presence of oxidized and reduced glutathione using the methods described previously for μ-SmIIIA (*11*). HPLC analysis of the folding reactions indicated the presence of one predominant product for each peptide (Figure 2B). After purification of this material on a reversed-phase C_{18} column, the peptides were analyzed by MADLI-TOF, yielding the expected molecular mass (monoisotopic): μ-SIIIA $[MH^+] = m/z$ 2206.9 (calculated $[MH^+] = m/z$ 2206.8) and μ-KIIIA $[MH^+] = m/z$ 1883.8 (calculated $[MH^+] = m/z$ 1883.6).

Comparison of the Activity of μ-Conotoxins SIIIA and KIIIA to That of Previously Characterized μ-Conotoxin SmIIIA. The electrophysiological experiments carried out previously to demonstrate the novel specificity of μ-SmIIIA for TTX-r VGSCs used dissociated neurons from frog sympathetic and sensory ganglia. We therefore assayed chemically synthesized μ-conotoxins SIIIA and KIIIA on TTX-r currents of these neurons (see Experimental Procedures). As shown in panels A and B of Figure 3, both μ-SIIIA and μ-KIIIA inhibited TTX-r currents in these neurons. The kinetics of the block by both peptides followed a single-exponential time course for sympathetic (Figure 3B, bottom) and DRG (not illustrated) neurons, just like the block by μ-SmIIIA (*11*). On DRG neurons, the observed rate constants (k_{obs}) for 1 μM μ-KIIIA and μ-SIIIA were 0.21 ± 0.02 min^{-1} ($N = 5$) and 0.10 ± 0.01 min^{-1} ($N = 4$), respectively. On sympathetic neurons, the respective rates were 0.28 ± 0.05 min^{-1} ($N = 3$) and 0.12 ± 0.01 min^{-1} ($N = 4$), respectively. For both types of neurons, μ-KIIIA blocked significantly faster than μ-SIIIA, and there was no significant difference in the k_{obs} values for each peptide on DRG versus sympathetic neurons (Student's *t*-test, $p < 0.05$).

The kinetics of block by both peptides of TTX-r currents in sympathetic neurons were scrutinized by examining their concentration dependence. The value of k_{obs} increased linearly as a function of concentration (Figure 3C). As previously observed for μ-SmIIIA (*11*), such results are consistent with a 1/1 interaction between the toxin and its TTX-r sodium channel target with kinetics described by the equation k_{obs}

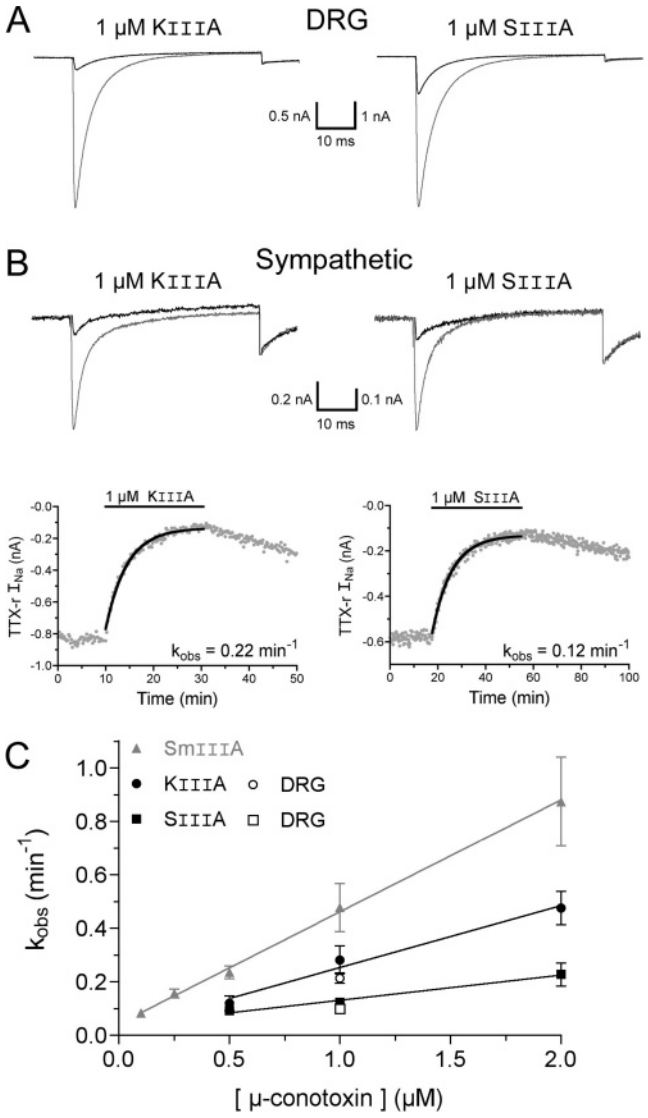

FIGURE 3: Comparison of effects of μ-conotoxins on TTX-resistant sodium currents. Dissociated frog DRG and sympathetic neurons were prepared as described in Experimental Procedures. Neurons were held at −80 mV, and a 50 ms test pulse to 0 mV was used. Each test pulse was preceded by a 50 ms prepulse to −120 mV to relieve steady-state inactivation. All traces represent the average of 10 responses, either in the absence (control traces, gray) or in the presence of 1 μM μ-conotoxin (black traces). (A) Representative TTX-resistant current traces recorded from DRG neurons following an ~55 min exposure to μ-KIIIA (left) or an ~30 min exposure to μ-SIIIA (right). (B) Representative TTX-resistant current traces (top) recorded from sympathetic neurons following an ~20 min exposure to μ-KIIIA (left) or μ-SIIIA (right). Peak amplitudes (bottom) of the TTX-resistant currents plotted as a function of time (gray points) and corresponding single-exponential best-fit curves (solid black lines). Horizontal black lines represent the times at which μ-conotoxin was present. Current traces were obtained every 10 s. (C) Observed rate constant (k_{obs}) vs μ-conotoxin concentration. Error bars represent SEM ($N = 3-5$ for each data point). The best-fit linear regression lines (solid lines) are shown for each toxin's block of TTX-r currents in sympathetic neurons (solid symbols); slope and intercept values are given in the Results. The k_{obs} values for block of TTX-r currents in DRG neurons by 1 μM μ-conotoxin are represented by empty symbols.

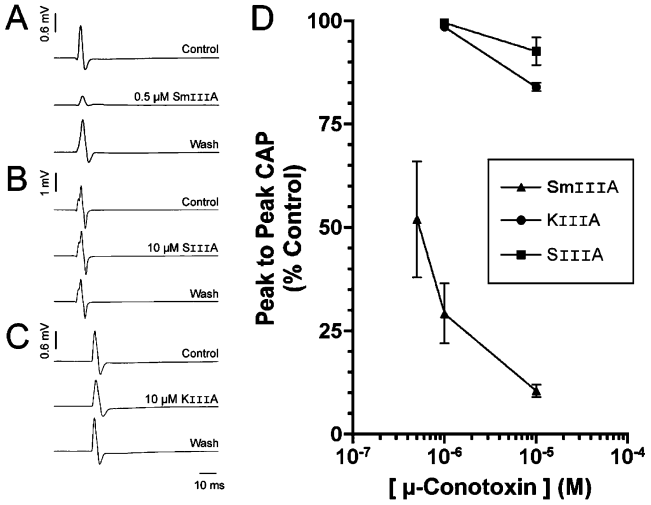

FIGURE 4: Compared to μ-SmIIIA, μ-conotoxins KIIIA and SIIIA are less potent inhibitors of frog skeletal muscle action potentials. Extracellular recording from frog nerve muscle preparations were performed as described in Experimental Procedures. (A−C) Representative traces of muscle CAPs evoked by indirect stimulation. In each panel, a representative trace in the presence of toxin is compared with control and wash traces. All toxin exposures were in a static bath. Note that 0.5 μM μ-SmIIIA (A) reversibly inhibited muscle CAPs, while 10 μM μ-conotoxins SIIIA (B) and KIIIA (C) produced relatively little block. (D) Dose−response relationships for inhibition of skeletal muscle CAPs. The peak-to-peak CAP amplitude, relative to that of control, was measured after 10 min exposures to varying concentrations of μ-conotoxin SmIIIA, SIIIA, or KIIIA. The averages of these measurements taken from multiple muscle preparations are plotted as a function of toxin concentration ($N = 2-5$). Error bars represent the SEM. At a concentration of 1 μM, a 10 min exposure to either μ-KIIIA ($N = 4$) or μ-SIIIA ($N = 2$) did not inhibit the muscle CAP, while μ-SmIIIA ($N = 4$) inhibited approximately 70% of the peak-to-peak amplitude.

$= k_{on}[\text{toxin}] + k_{off}$. The on-rate constants (k_{on}) obtained from the slopes of the linear regression lines in Figure 3C were $0.23 \pm 0.04\ \mu M^{-1}\ min^{-1}$ for μ-KIIIA and $0.09 \pm 0.02\ \mu M^{-1}\ min^{-1}$ for μ-SIIIA. These are significantly different from each other and slower than the k_{on} for μ-SmIIIA of $0.42 \pm 0.04\ \mu M^{-1}\ min^{-1}$. The off-rate constants (k_{off}) obtained from the *Y*-intercepts of the lines in Figure 3C were $0.02 \pm 0.06\ min^{-1}$ for μ-KIIIA and 0.04 ± 0.03 for μ-SIIIA. Although these values were not significantly different from zero, the block by μ-KIIIA and μ-SIIIA was clearly, albeit slowly, reversible following toxin washout (Figure 3, bottom), unlike the block by μ-SmIIIA, which showed no signs of reversal over a similar wash period (e.g., see Figure 5 in ref *12*).

We also compared the effects of μ-conotoxins SIIIA and KIIIA with each other and with that of μ-SmIIIA on frog skeletal muscle CAPs evoked by indirect stimulation. The results of these experiments are shown in Figure 4. Panels A−C illustrate representative responses, and dose−response curves for the three peptides are illustrated in panel D.

While a 10 min application of 0.5 μM μ-SmIIIA reversibly inhibited the muscle CAP, either μ-SIIIA or μ-KIIIA at 10 μM had minimal effects. However, at >10 μM, both μ-SIIIA and μ-KIIIA reversibly inhibited muscle CAPs (not shown). These data are summarized in Figure 4D. It is apparent that μ-SIIIA and μ-KIIIA are much less potent inhibitors of frog skeletal muscle VGSCs than μ-SmIIIA. These results indicate that the two new peptides are better than μ-SmIIIA in discriminating between TTX-r VGSCs and the (TTX-sensitive) skeletal muscle subtype.

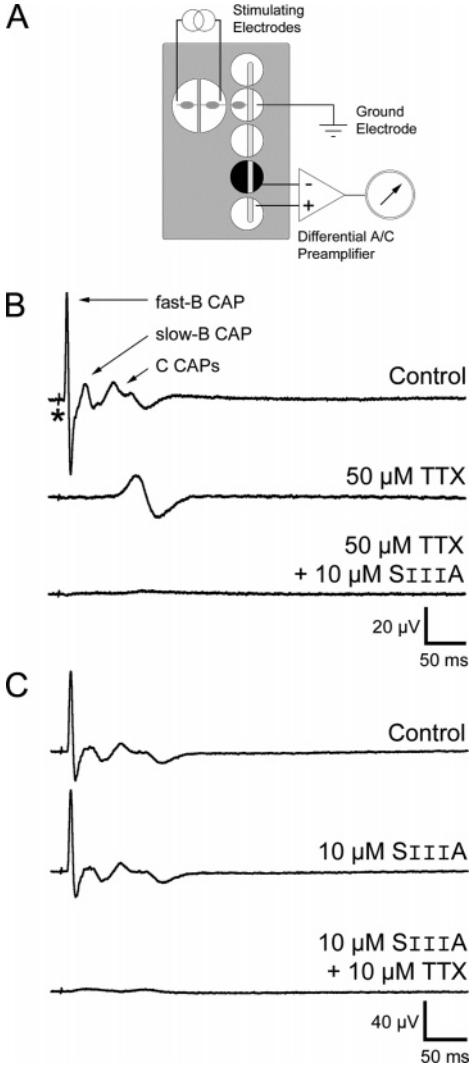

FIGURE 5: Effects of μ-SIIIA and TTX on B- and C-neuron CAPs in the postganglionic sympathetic nerve of frog. Recordings were made as described in Experimental Procedures. (A) Sketch of the sympathetic preparation and arrangement of stimulating and recording electrodes. Shaded ovals represent ganglia. Toxins were applied to the test compartment (darkened well) that contained a segment of the 10th spinal nerve (shaded vertical line spanning five wells). (B) CAPs in control Ringer's solution (top), in the presence of 50 μM TTX (middle), or in the presence of 50 μM TTX and 10 μM μ-SIIIA (bottom). (C) CAPs in control solution (top), in the presence of 10 μM SIIIA (middle), or in the presence of 10 μM SIIIA and 10 μM TTX (bottom). Each trace represents the average of 10 responses. The asterisk indicates the stimulus artifact. TTX-sensitive fast and slow B-neuron CAPs were largely unaffected by μ-SIIIA. Although C-neuron CAPs were slowed, they were not blocked by TTX. μ-SIIIA did not affect C-neuron CAPs unless TTX was also present; thus, the presence of both toxins was required for elimination of C-neuron CAPs.

Previously, we reported that in frog sympathetic nerves μ-conotoxin SmIIIA inhibits C-neuron CAPs that persist in TTX (*12*). Figure 5 shows that μ-SIIIA produced similar effects in this preparation. CAPs were recorded from postganglionic sympathetic axons in the 10th spinal nerve in response to stimulation of preganglionic axons in the sympathetic chain, as illustrated in the sketch in Figure 5A. Fast and slow B-neuron CAPs were abolished by 50 μM TTX, but C-neuron CAPs were spared (Figure 5B). As shown previously (*12*), TTX slows the conduction velocity of the C-CAP and causes its two components to merge, resulting in a C-CAP that can be larger than in control, as

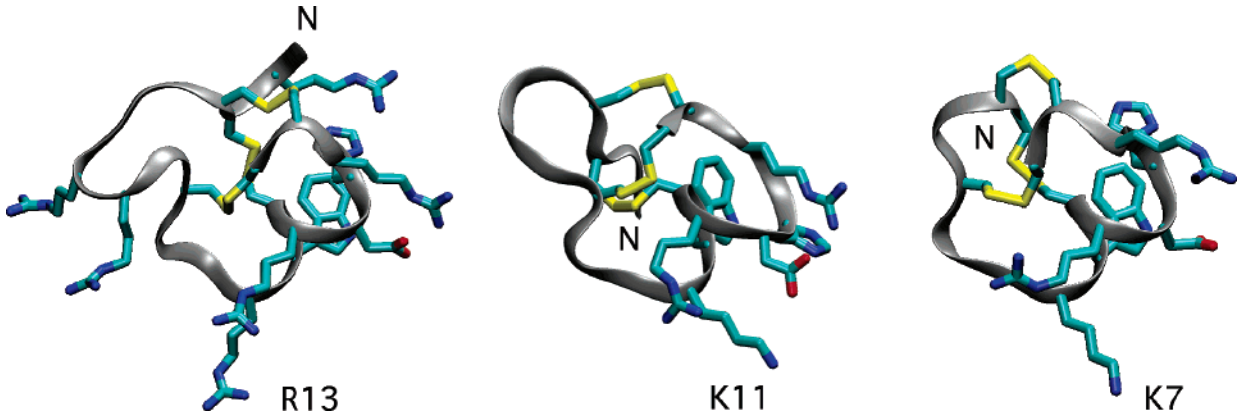

FIGURE 6: Ribbon diagrams of μ-conotoxins SmIIIA (left), SIIIA (middle), and KIIIA (right) from MD simulations after 10 ns. The side chains of all ionizable residues, as well as Cys, Trp, and His, are represented as tubes. The figure was generated using VMD (Visual Molecular Dynamics) software (*27*).

was the case here. When TTX was supplemented with 10 μM μ-SIIIA, the C-neuron CAP was abolished. In Figure 5C, the order of addition of the toxins was reversed. When μ-SIIIA (10 μM) was added alone, it had no apparent effects on either B- or C-neuron CAPs. However, when μ-SIIIA was supplemented with 10 μM TTX, both B- and C-neuron CAPs were abolished. Since neither B- nor C-neuron CAPs were affected by μ-SIIIA alone, this confirms that the TTX-sensitive VGSCs expressed in these neurons are largely resistant to μ-conotoxin SIIIA. Further, this indicates that the axons of C-neurons express sufficient levels of both TTX-sensitive and TTX-resistant VGSCs to allow action potentials to be propagated when either (but not both) type of channel is blocked.

Structural Consequences of Shortening the Loop Size in μ-SIIIA and μ-KIIIA. Molecular dynamics simulations were performed to gain insight into the potential structural consequences of deleting a number of residues in the first loop, i.e., the region flanked by the second and third Cys residues. The models of μ-SIIIA and μ-KIIIA, along with the structure of μ-SmIIIA resulting from MD simulation, are presented in Figure 6. The simulated structure of μ-SmIIIA shows several differences from the structure obtained from the NMR analysis. In particular, the side chain of Arg2 moves away from that of Trp14, in conflict with the observed NOEs between side chains of these residues (*12*). Extended simulations lasting 50 ns (see the Supporting Information) showed that the region containing the first loop (between Asn5 and Gly9) in the MD model sampled a larger region of conformational space than that consistent with the NMR-derived structure. Apart from these differences, the rest of the backbone was largely constant throughout the simulation, and consistent with the NMR structure. Significantly, the side chain groups of the ionizable residues and that of tryptophan and histidine occupy similar positions in the NMR and MD model structures of μ-SmIIIA.

The side chains of Trp14, Arg16, Asp17, and Arg20 occupy very similar spatial positions in all three μ-conotoxins, conferred by maintenance of the structure of the second and third loops through the formation of a short helical segment from Arg13 through Cys15, and Asp17 through Ser19 (μ-SmIIIA numbering). Comparison of the three structures in Figure 6 shows that the length of the first loop is predicted to have little effect on the overall structure, which is presumably determined largely by the disulfide bonding arrangement and the helical region discussed above.

DISCUSSION

We used a combination of molecular cloning and chemical synthesis to characterize two novel μ-conotoxins that exhibited unprecedented selectivity for TTX-r sodium currents. We had anticipated that these peptides might block TTX-r Na^+ current on the basis of their primary amino acid sequence, the sequence of which was more similar to that of *C. stercusmuscarum* μ-SmIIIA than to those of the muscle-specific peptides, μ-conotoxins GIIIA and PIIIA. A sequence comparison of all five toxins, including the peptides that block TTX-r sodium current as well as those that do not, is shown in Table 1.

One unusual and divergent sequence feature of the new peptides is the length of the first loop. In all previously characterized μ-conotoxins (PIIIA, GIIIA−C, and SmIIIA), there are five residues between the second and third Cys; in μ-SIIIA, there are only three, and most strikingly, in μ-KIIIA, there is only one. This surprising variability in the number and composition of AA residues in the first loop in biologically active μ-conotoxins, all of which block some molecular isoform of the family of VGSCs, was unexpected. The deletion of residues in the first loop of μ-conotoxins SIIIA and KIIIA without a significant change in their biological activity on the TTX-r VGSC is in contrast to a general observation that the loop sizes are found to be rather conserved among conotoxins belonging to individual families. To the best of our knowledge, this is the first example of such length variation of a conotoxin scaffold. Variation in the size of the first loop, such as that seen between μ-conotoxins SmIIIA and KIIIA, may be viewed as another mechanism for generating molecular diversity of conotoxins.

A second notable sequence feature of μ-SIIIA and μ-KIIIA is that the usually conserved arginine residue (designated with an arrow in Table 1) is replaced with Lys in both peptides. The extensive structure−function work that has been carried out on μ-GIIIA suggested that this Arg residue is important for the potency of this peptide (*23*−*25*). An R13K mutation in μ-conotoxin GIIIA resulted in a more than 10-fold decrease in its ability to block skeletal muscle VGSCs (*23*−*25*). Thus, such a Lys substitution at this otherwise conserved locus in natural μ-conotoxins was surprising.

The characterization of the new conopeptides provides valuable leads for defining the important factors in subtype

selectivity for various VGSCs. A preliminary study on chimeras of various μ-conotoxins has demonstrated that it is the C-terminal amino acids, highly conserved among μ-SmIIIA, μ-SIIIA, and μ-KIIIA in the second and third loop, that are responsible for activity on TTX-r VGSCs, although precisely which specific amino acids are important for potency remain to be identified (*12*). Not surprisingly, the C-terminal regions are predicted to be almost fully conserved in terms of structure as well (Figure 6), consistent with the proposed role of this region in selectivity for TTX-r channels, as suggested by Keizer et al. (*12*). Thus, even though the structures shown in Figure 6 are models based on molecular dynamics simulations, they suggest that the surface associated with the C-terminal region, in particular, Trp12 and His16 of μ-SIIIA (Trp8 and His12, respectively, in μ-KIIIA), may play a key role in binding to TTX-r channels.

Structural features that may contribute to the ability of μ-conotoxins SIIIA and KIIIA to discriminate between TTX-r and skeletal muscle VGSCs compared to μ-SmIIIA are the smaller first loop in μ-SIIIA and μ-KIIIA, the amino acid composition of this loop (two vicinal Arg residues present in μ-SmIIIA are absent in μ-SIIIA and μ-KIIIA), the Arg to Lys substitution in the second loop, or a combination of these features. A detailed structure−function study of these peptides has been initiated, as well as a discovery project to identify additional natural μ-conotoxins that might preferentially target TTX-r VGSCs.

ACKNOWLEDGMENT

We thank Jacob S. Nielsen for his assistance with chemical synthesis of the peptides and Brad Green for mass spectrometry analysis.

NOTE ADDED AFTER PRINT PUBLICATION

The name of author Maren Watkins was incorrect in the version published on the Web 04/21/05 (ASAP) and in the May 17, 2005, issue (Vol. 44, No. 19, pp 7259−7265). The corrected electronic version was published 02/08/06, and an Addition and Correction appears in the March 7, 2006, issue (Vol. 45, No. 9).

SUPPORTING INFORMATION AVAILABLE

One figure documenting a 50 ns molecular dynamics simulation of μ-conotoxin SmIIIA. This material is available free of charge via the Internet at http://pubs.acs.org.

REFERENCES

1. Catterall, W. A. (2000) From ionic currents to molecular mechanisms: The structure and function of voltage-gated sodium channels, *Neuron 26*, 13−25.
2. Goldin, A. L. (2001) Resurgence of sodium channel research, *Annu. Rev. Physiol. 63*, 871−894.
3. Hille, B. (2001) *Ion Channels of Excitable Membranes*, 3rd ed, Sinauer Associates, Sunderland, MA.
4. Wood, J. N., Boorman, J. P., Okuse, K., and Baker, M. D. (2004) Voltage-gated sodium channels and pain pathways, *J. Neurobiol. 61*, 55−71.
5. Terlau, H., and Olivera, B. M. (2004) *Conus* venoms: A rich source of novel ion channel-targeted peptides, *Physiol. Rev. 84*, 41−68.
6. Cestele, S., and Catterall, W. A. (2000) Molecular mechanisms of neurotoxin action on voltage-gated sodium channels, *Biochimie 82*, 883−892.
7. Cruz, L. J., Gray, W. R., Olivera, B. M., Zeikus, R. D., Kerr, L., Yoshikami, D., and Moczydlowski, E. (1985) *Conus geographus* toxins that discriminate between neuronal and muscle sodium channels, *J. Biol. Chem. 260*, 9280−9288.
8. Shon, K., Olivera, B. M., Watkins, M., Jacobsen, R. B., Gray, W. R., Floresca, C. Z., Cruz, L. J., Hillyard, D. R., Bring, A., Terlau, H., and Yoshikami, D. (1998) μ-Conotoxin PIIIA, a new peptide for discriminating among tetrodotoxin-sensitive Na channel subtypes, *J. Neurosci. 18*, 4473−4481.
9. Safo, P., Rosenbaum, T., Shcherbatko, A., Choi, D., Han, E., Toledo-Aral, J., Olivera, B. M., Brehm, P., and Mandel, G. (2000) Distinction among neuronal subtypes of voltage-activated sodium channels by μ-conotoxin PIIIA, *J. Neurosci. 20*, 76−80.
10. Nielsen, K. J., Watson, M., Adams, D. J., Hammarström, A. K., Gage, P. W., Hill, J. M., Craik, D. J., Thomas, L., Adams, D., Alewood, P. F., and Lewis, R. J. (2002) Solution structure of μ-conotoxin PIIIA, a preferential inhibitor of persistent tetrodotoxin-sensitive sodium channels, *J. Biol. Chem. 277*, 27247−27255.
11. West, P. J., Bulaj, G., Garrett, J. E., Olivera, B. M., and Yoshikami, D. (2002) μ-Conotoxin SmIIIA, a potent inhibitor of TTX-resistant sodium channels in amphibian sympathetic and sensory neurons, *Biochemistry 41*, 15388−15393.
12. Keizer, D. W., West, P. J., Lee, E. F., Yoshikami, D., Olivera, B. M., Bulaj, G., and Norton, R. S. (2003) Structural basis for tetrodotoxin-resistant sodium channel binding by μ-conotoxin SmIIIA, *J. Biol. Chem. 278*, 46805−46813.
13. Jones, S. W. (1987) Sodium currents in dissociated bull-frog symapthetic neurones, *J. Physiol. 389*, 605−627.
14. Selyanko, A. A., Smith, P. A., and Zidichouski, J. A. (1990) Effects of muscarine and adrenaline on neurones from *Rana pipiens* sympathetic ganglia, *J. Physiol. 425*, 471−500.
15. Yoshikami, D., Bagabaldo, Z., and Olivera, B. M. (1989) The inhibitory effects of ω-conotoxins on calcium channels and synapses, *Ann. N.Y. Acad. Sci. 560*, 230−248.
16. Tavazoie, S. F., Tavazoie, M. F., McIntosh, J. M., Olivera, B. M., and Yoshikami, D. (1997) Differential block of nicotinic synapses on B vs. C neurones in sympathetic ganglia of frog by α-conotoxins MII and ImI, *Br. J. Pharmacol. 120*, 995−1000.
17. Martí-Renom, M. A., Stuart, A., Fiser, A., Sanchez, R., Melo, F., and Sali, A. (2000) Comparative protein structure modelling of genes and genomes, *Annu. Rev. Biophys. Biomol. Struct. 29*, 291−325.
18. Fiser, A., and Sali, A. (2003) Modeller: Generation and refinement of homology-based protein structure models, *Methods Enzymol. 374*, 463−493.
19. Lindahl, E., Hess, B., and van der Spoel, D. (2001) Gromacs 3.0: A package for molecular simulation and trajectory analysis, *J. Mol. Model. 7*, 306−317.
20. Jorgensen, W. L., and Tirado-Rives, J. (1988) The OPLS potential functions for proteins. Energy minimizations for crystals of cyclic peptides and crambin, *J. Am. Chem. Soc. 110*, 1657−1666.
21. Hess, B., Bekker, H., and Berendsen, H. J. C. (1977) LINCS: A linear constraint solver for molecular simulations, *J. Comput. Chem. 18*, 1463−1472.
22. Berendsen, H. J. C., Postma, J. P. M., DiNola, A., and Haak, J. R. (1984) Molecular dynamics with coupling to an external bath, *J. Chem. Phys. 81*, 3684−3690.
23. Chang, N. S., French, R. J., Lipkind, G. M., Fozzard, H. A., and Dudley, S., Jr. (1998) Predominant interactions between μ-conotoxin Arg-13 and the skeletal muscle Na^+ channel localized by mutant cycle analysis, *Biochemistry 37*, 4407−4419.
24. Nakamura, M., Niwa, Y., Ishida, Y., Kohno, T., Sato, K., Oba, Y., and Nakamura, H. (2001) Modification of Arg-13 of μ-conotoxin GIIIA with piperidinyl-Arg analogs and their relation to the inhibition of sodium channels, *FEBS Lett. 503*, 107−110.
25. Hui, K., Lipkind, G., Fozzard, H. A., and French, R. J. (2002) Electrostatic and steric contributions to block of the skeletal muscle sodium channel by μ-conotoxin, *J. Gen. Physiol. 119*, 45−54.
26. Cruz, L. J., Kupryszewski, G., LeCheminant, G. W., Gray, W. R., Olivera, B. M., and Rivier, J. (1989) μ-Conotoxin GIIIA, a peptide ligand for muscle sodium channels: Chemical synthesis, radiolabeling and receptor characterization, *Biochemistry 28*, 3437−3442.
27. Humphrey, W., Dalke, A., and Schulten, K. (1996) VMD: Visual molecular dynamics, *J. Mol. Graphics 14*, 33−38.

BI0473408